15 January 2002

ELSEVIER

Optics Communications 201 (2002) 373–380

OPTICS COMMUNICATIONS

www.elsevier.com/locate/optcom

Dynamical quantum statistical effects in optical parametric processes

M.K. Olsen [a,*], L.I. Plimak [b], A.Z. Khoury [a]

[a] *Instituto de Física da Universidade Federal Fluminense, Boa Viagem Cep.: 24210-340, Niterói, Rio de Janeiro, Brazil*
[b] *Fachbereich Physik, Universität Kaiserslautern, 67663 Kaiserslautern, Germany*

Received 16 October 2001; received in revised form 21 November 2001; accepted 28 November 2001

Abstract

We investigate the dynamical and statistical effects of different input states of the electromagnetic field in the travelling wave parametric processes of second harmonic generation and nondegenerate downconversion. Using the phase space techniques of stochastic integration in the positive-P representation, equivalent to a fully quantum mechanical analysis, we consider different input states and show that the effects on the mean field solutions can be quite drastic. We also investigate the effects of the input statistics on the quantum properties of the output fields, finding that a thermal input can actually cause the value of some quantum correlations to increase.

PACS: 42.50.Ct; 42.50.Ar; 42.65.-k; 42.65.Ky

Keywords: Quantum optics; Quantum correlations; Fully quantum analysis

1. Introduction

Among the simplest possible quantum optical systems which exhibit nonclassical behaviour are travelling wave second harmonic generation and parametric downconversion. These processes couple modes of the electromagnetic field with different frequencies via a nonlinear medium and are well known for the production of nonclassical states of the electromagnetic field. Both systems have been treated theoretically using various levels of approximation, from a classical analysis of the interacting fields [1], linearisation of the operator equations of motion for the fields [2–4] and linearisation of the operator equations for the intensities [5,6]. A common approximation for the optical parametric oscillator is to treat the pump field as remaining undepleted as it traverses the crystal [7–9], which leads to solutions for the fields which clearly violate energy conservation as well as over optimistic predictions for the quantum features of the fields [6,10], predicting, for example, that the violation of quantities such as Bell's inequalities will increase with the conversion parameter. Another approach is to diagonalise the interaction

* Corresponding author. Tel.: +55-21-2620-6735; fax: +55-21-2620-3881.
E-mail address: mko@if.uff.br (M.K. Olsen).

0030-4018/02/$ - see front matter
PII: S0030-4018(01)01711-4

Hamiltonian [11], which results in equations which can be solved numerically for small photon numbers. A series expansion of the time evolution operator has also been used to evolve the initial state vector [12], as well as a perturbation expansion of solutions for the Heisenberg equations of motion, valid for smallish times and arbitrary photon numbers [13], but with numerical results for small photon numbers. The distribution of the Q-function in phase space has been investigated analytically for arbitrary field intensities [14], the applicability of the nondepleted pump approximation has been analysed [15] and the Wigner function and the maximum of the pump depletion have been calculated [16], using the classical solutions of [1], with results that should in principle become more valid as the photon number increases.

In this paper we treat the interacting fields using phase space methods, focussing on the effects of different input states on both the dynamics and the output statistics. Although we must proceed numerically, we are not in principle limited as to the field intensities and interaction lengths that we may consider. A great advantage of this method is that the resulting stochastic equations are fully equivalent to the master equation, so that we are not making any approximations to find the time development of the system. For input states which have well behaved Glauber P-functions [17,18], we may use the positive-P representation [19]. It is of interest to mention here that in this case the choice of representation is a matter of taste, as all the operator products we calculate can equally well be calculated in the truncated Wigner representation, with the same results being found. This is an indication that the Wigner function for these processes may remain positive, starting with input states with a positive Wigner distribution.

Although the effects of pump fluctuations have previously been calculated for the nondegenerate optical parametric amplifier (NOPA) [9], this was done in the nondepleted pump approximation, using a classical type distribution for the pumping parameter and taking averages over the resulting semi-classical solutions. What we do here is represent fluctuations in the inputs by their pseudo-probability functions, ensuring that we are calculating the correct quantum properties. In the stimulated nondegenerate optical parametric amplifier (SNOPA), we consider different states of the auxiliary input which stimulates the process. In travelling wave second harmonic generation, we consider different states of the input at the fundamental frequency. In both cases we find that a thermal input can drastically affect the dynamics as well as the statistics of the converted modes.

2. Nondegenerate optical parametric amplifier

Parametric downconversion, achieved via an optical parametric amplifier (OPA), is of special interest because it allows for experiments concerned with the fundamentals of quantum mechanics. Among these are violations of Bell's inequalities [20,21] and preparation of Einstein–Podolsky–Rosen states [4,10,22]. We will consider two cases here: one where two vacuum fields are amplified, and one where there is a nonvacuum input field at one of the downconverted frequencies.

The system of interest couples three electromagnetic fields via a nonlinear medium (normally a crystal), with a second-order susceptibility represented by κ. The three fields are represented at position z inside the crystal by the bosonic annihilation operators $\hat{a}(z)$, $\hat{b}(z)$ and $\hat{c}(z)$, with respective frequencies ω_a, ω_b and ω_c, such that $\omega_a + \omega_b = \omega_c$. Generally the fields at $z = 0$ may take on a range of values, corresponding to different physical processes. In this paper we consider only the case of perfect phase matching and colinear propagation without dispersion, so that we may write the effective interaction Hamiltonian as

$$H = \frac{i\hbar\kappa}{2}\left[\hat{a}^\dagger\hat{b}^\dagger\hat{c} - \hat{a}\hat{b}\hat{c}^\dagger\right], \tag{1}$$

from which, following the usual methods and using Itô calculus [23], we find the following set of coupled stochastic differential equations in the positive-P representation, where there is a correspondence between the variables $(\alpha, \alpha^+, \beta, \beta^+, \gamma, \gamma^+)$ and the operators $(\hat{a}, \hat{a}^\dagger, \hat{b}, \hat{b}^\dagger, \hat{b}, \hat{b}^\dagger)$:

$$
\begin{aligned}
\frac{d\alpha}{dz} &= \frac{\kappa}{2}\beta^{+}\gamma + \frac{1}{2}\sqrt{\kappa\gamma}(\eta_1(z) + i\eta_2(z)),\\
\frac{d\alpha^{+}}{dz} &= \frac{\kappa}{2}\beta\gamma^{+} + \frac{1}{2}\sqrt{\kappa\gamma^{+}}(\eta_3(z) + i\eta_4(z)),\\
\frac{d\beta}{dz} &= \frac{\kappa}{2}\alpha^{+}\gamma + \frac{1}{2}\sqrt{\kappa\gamma}(\eta_1(z) - i\eta_2(z)),\\
\frac{d\beta^{+}}{dz} &= \frac{\kappa}{2}\alpha\gamma^{+} + \frac{1}{2}\sqrt{\kappa\gamma^{+}}(\eta_3(z) - i\eta_4(z)),\\
\frac{d\gamma}{dz} &= -\frac{\kappa}{2}\alpha\beta,\\
\frac{d\gamma^{+}}{dz} &= -\frac{\kappa}{2}\alpha^{+}\beta^{+}.
\end{aligned}
\tag{2}
$$

In the above, the η_i are real noise terms with the correlations $\overline{\eta_i(z)\eta_j(z')} = \delta_{ij}\delta(z-z')$. As always with the positive-P, the pairs of field variables (α and α^{+} for example) are not complex conjugate except in the mean of a large number of integrated trajectories. We are particularly interested here in a system where $\gamma(0) \neq 0$ and $\alpha(0) = 0$, but $\beta(0) \neq 0$, and in which we consider the effects of different quantum states for $\beta(0)$, the auxiliary signal field. Unlike the treatment of [9], the fluctuations in the pump field as it traverses the crystal are automatically taken into account in our treatment. In what follows, we will always use the values $\kappa = 0.01$ and $\overline{|\gamma(0)|^2} = 10^6$, and the scaled dimensionless interaction parameter $\xi = \kappa|\gamma(0)|z$.

2.1. Coherent pump fluctuations

Before we consider the effects of different input states of the signal, let us examine the fluctuations in intensity of the pump field as it traverses the crystal, as well as the correlation in intensity between the two downconverted modes. In [9], the pump is treated as being a fluctuating quantity with a constant mean value, and a standard deviation which grows linearly in time. In contrast to this, we treat the pump field as being initially in a coherent state and investigate the change in its statistics due to the interaction with the nonlinear medium.

To this end we have calculated the Fano factor:

$$
F(N_c) = \frac{\langle :(\hat{c}^{\dagger}\hat{c})^2: \rangle - \langle \hat{c}^{\dagger}\hat{c} \rangle^2}{\langle \hat{c}^{\dagger}\hat{c} \rangle} \tag{3}
$$

of this field as it traverses the crystal. A coherent state, being an example of a field which obeys a Poissonian intensity distribution, has a value of 1 for this factor. What we can see from Fig. 1 is that the pump field remains Poissonian over an appreciable interaction length. As can be seen by comparison with [6], this field begins to exhibit super-Poissonian statistics at around the value of ξ that it begins to be noticeably depleted. There is an initial plateau where the Fano factor does not change at all, which actually extends past the range of experimentally reasonable interaction strength. The statistics only change when upconversion begins to play a role. What is obvious from this graph is that the increased fluctuations do not follow the form supposed in [9]. Also shown in Fig. 1 is the correlation coefficient of the intensities of the two downconverted modes:

$$
\rho(N_a, N_b) = \frac{\langle \hat{a}^{\dagger}\hat{a}\hat{b}^{\dagger}\hat{b} \rangle - \langle \hat{a}^{\dagger}\hat{a} \rangle \langle \hat{b}^{\dagger}\hat{b} \rangle}{V(N_a)V(N_b)}, \tag{4}
$$

which we have used rather than the normalised correlation of [9], as a value of 1 demonstrates a perfect correlation between the two intensities [24].

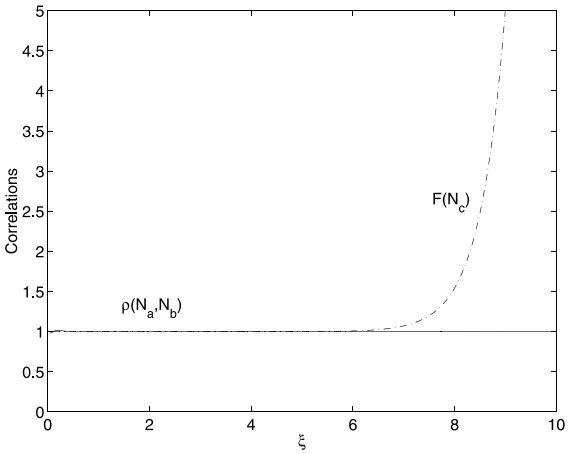

Fig. 1. The Fano factor ($F(N_c)$) of the pump field and the intensity correlation coefficient ($\rho(N_a, N_b)$) of the two downconverted modes as they traverse the crystal in the spontaneous case. The pump field has the value $|\gamma(0)|^2 = 10^6$. The horizontal axis is in units of the normalised interaction strength, $\xi = \kappa|\gamma(0)|z$. This plot is the result of 3.5×10^5 stochastic trajectories. All values plotted in this and subsequent graphics are dimensionless.

What we immediately see is that these two fields are perfectly correlated in intensity over the interaction range considered, which is to be expected as the downconverted photons can only be created in pairs.

2.2. Thermal signal input

One method of increasing the conversion efficiency of the NOPA is to inject a signal field at one of the lower frequencies, resulting in a process of stimulated photon pair production. We have shown in an earlier paper [6] that with a coherent signal there is necessarily some loss of the quantum properties of the output fields as the signal intensity is increased. To this end we calculated the degree of violation of a coefficient based on the Cauchy–Schwarz inequality:

$$\langle \hat{a}^{\dagger 2}\hat{a}^2\rangle\langle \hat{b}^{\dagger 2}\hat{b}^2\rangle \geqslant \langle \hat{a}^{\dagger}\hat{a}\hat{b}^{\dagger}\hat{b}\rangle^2, \tag{5}$$

which may not be violated by fields with a positive P-function, and hence any violation may be thought of as a measure of the quantum nature of the two fields. Rewriting this as a correlation function, we have

$$\frac{\langle \hat{a}^{\dagger 2}\hat{a}^2\rangle\langle \hat{b}^{\dagger 2}\hat{b}^2\rangle}{\langle \hat{a}^{\dagger}\hat{a}\hat{b}^{\dagger}\hat{b}\rangle^2} \geqslant 1, \tag{6}$$

so that any value of less than one indicates nonclassical behaviour. Other properties of interest are the cross-mode correlations

$$g^{(2)}(\hat{a},\hat{b},0) = \frac{\langle \hat{a}^{\dagger}\hat{a}\hat{b}^{\dagger}\hat{b}\rangle}{\langle \hat{a}^{\dagger}\hat{a}\rangle\langle \hat{b}^{\dagger}\hat{b}\rangle}, \tag{7}$$

which gives a measure of coincidence counts in the two lower frequency modes, and

$$g^{(4)}(\hat{a},\hat{b},0) = \frac{\langle \hat{a}^{\dagger 2}\hat{a}^2\hat{b}^{\dagger 2}\hat{b}^2\rangle}{\langle \hat{a}^{\dagger}\hat{a}\rangle^2\langle \hat{b}^{\dagger}\hat{b}\rangle^2}, \tag{8}$$

which measures the probability of simultaneously detecting two photons in each mode.

To model a thermal input signal with the same mean intensity as the coherent signal, we choose the initial condition for each stochastic trajectory according to the P-distribution for a thermal state:

$$P(\beta) = \frac{1}{\pi\bar{n}}\exp(-|\beta|^2/\bar{n}), \tag{9}$$

where $\bar{n}$ corresponds to the mean photon number and each β so chosen has a random phase, as a thermal state has no phase information. This means that the initial condition for each trajectory of the stochastic integration becomes $\beta(0) = [\beta^{\dagger}(0)]^*$, distributed in accord with the probability of Eq. (9).

In Fig. 2 we show the mean values of the idler field for coherent pumping ($|\gamma(0)|^2 = 10^6$), and coherent and thermal signal fields with a mean value of $|\beta(0)|^2 = 100$. What is immediately obvious is that the thermal signal results in less peak conversion efficiency on average, but we also need to consider fluctuations in the idler output. Examining Fig. 3, we see that, although in both cases the intensity fluctuations are huge (remember that the Fano factor for a coherent state is 1), with a thermal signal the variance is noticeably larger. This suggests that the idler field will be fluctuating wildly in intensity, with statistics which are essentially those of a thermal state, in which the Fano factor is equal to the mean photon number. When we examine the Cauchy–Schwarz correlation of Eq. (6) for these two cases, as shown in Fig. 4, we see that the violation is minimal, even with a coherent signal 10^4 times weaker than the pump, and

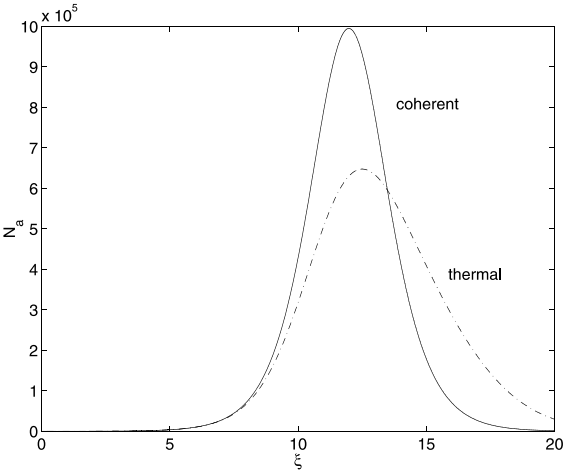

Fig. 2. The mean photon number in the idler. The coherent result is for an injected coherent signal with $|\beta(0)|^2 = 10^2$ while the thermal result has the same mean intensity in the signal. Both use a coherent pump with $|\gamma(0)|^2 = 10^6$. The coherent result used 7×10^4 stochastic trajectories and the thermal result used 3.3×10^5.

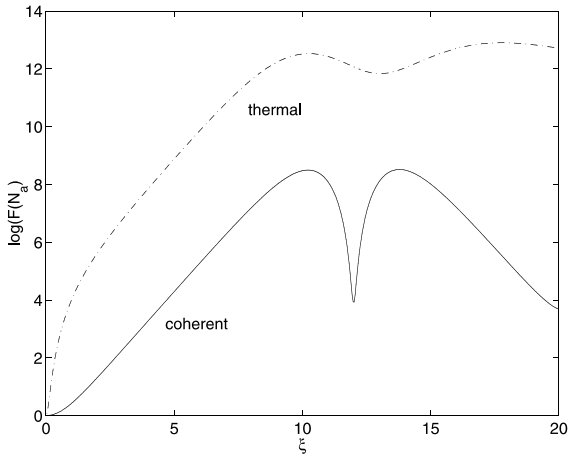

Fig. 3. The Fano factors of the idler, with coherent and thermal signals as in Fig. 2. Note that the factors are plotted on a logarithmic scale.

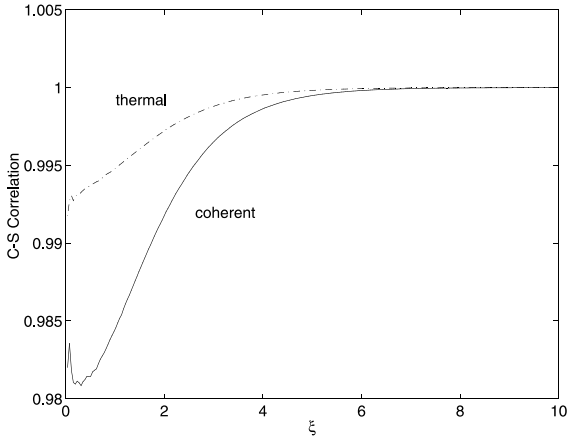

Fig. 4. The values for the Cauchy–Schwarz coefficient, for coherent and thermal signals, as in Fig. 2.

is even smaller with the thermal input. This is to be expected as the thermal input is more classical than a coherent state and therefore less able to help generate fields which violate classical inequalities. We note here that calculations using the truncated Wigner representation give essentially the same results for the violation of this inequality, demonstrating that it may also be explained using the semiclassical theory of stochastic electrodynamics.

However, when we examine the coincidence coefficients of Eqs. (7) and (8), as shown in Fig. 5, we see that a thermal signal generates much higher likelihoods of simultaneously detecting either one or two photons in each lower frequency field. This is to be expected, as the increase in generation of photons in the idler with an added signal is a stimulated process, depending on the intensity, and there is a much higher likelihood of finding high intensity fluctuations (photon bunching) with a thermal signal than with a coherent one. It is precisely these fluctuations which can generate production of pairs and double pairs. This phenomenon could conceivably be useful for the production of GHZ states [25–27], although the signal field would probably need to be of the same frequency as the idler so as to enable indistinguishability of the paths. In [26,27], spontaneous double pairs are created by passing a pulsed laser two times through a crystal. Detection of one of the photons leaves the other three in a GHZ state, although there are some problems with the visibility of the resulting measurements. Whether an injected thermal, or even semi-thermal signal could result in higher efficiency production and detection of these states is a subject for further investigation, outside the scope of this paper.

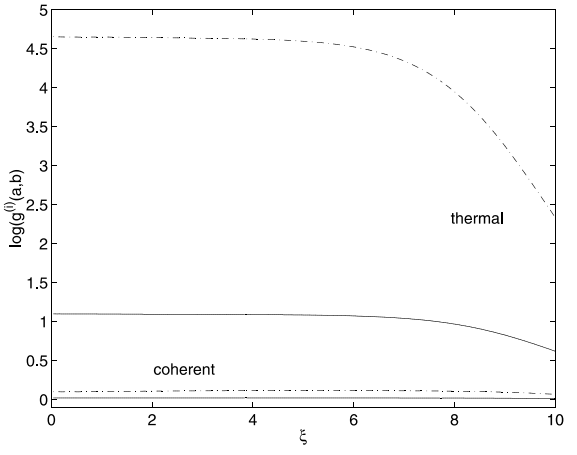

Fig. 5. The values for the coefficients $g^{(2)}(\hat{a},\hat{b},0)$ (solid lines) and $g^{(4)}(\hat{a},\hat{b},0)$ (dash–dotted lines), for coherent and thermal signals, as in Fig. 2. Note that the coefficients are plotted on a logarithmic scale.

3. Travelling wave second harmonic generation

We consider a nonlinear, phase-matched $\chi^{(2)}$ crystal, in which a plane-wave field at the fundamental frequency ω produces an harmonic field at frequency 2ω. In the travelling wave regime we can write an interaction Hamiltonian, with the trivial ω dependence of the fields removed, as

$$H = \frac{i\hbar\kappa}{2}\left[\hat{a}^{\dagger 2}\hat{b} - \hat{a}^2\hat{b}^{\dagger}\right], \tag{10}$$

where $\hat{a}$ and $\hat{b}$ are the annihilation operators for photons at frequencies ω and 2ω, respectively, at position z inside the nonlinear crystal, and κ represents the effective strength of the nonlinear interaction between the two modes. Again using the usual methods [23], this system can be mapped exactly onto stochastic partial differential positive-P equations (note that we are using Itô calculus), via the master and Fokker–Planck equations, resulting in

$$\begin{aligned}
\frac{d\alpha}{dz} &= \kappa\alpha^{+}\beta + \sqrt{\kappa\beta}\eta_1(z),\\
\frac{d\alpha^{+}}{dz} &= \kappa\alpha\beta^{+} + \sqrt{\kappa\beta^{+}}\eta_2(z),\\
\frac{d\beta}{dz} &= -\frac{\kappa}{2}\alpha^2,\\
\frac{d\beta^{+}}{dz} &= -\frac{\kappa}{2}\alpha^{+2},
\end{aligned} \tag{11}$$

where the noise terms $\eta_j(z)$ are real and Gaussian such that

$$\overline{\eta_j(z)\eta_k(z')} = \delta_{jk}\delta(z - z'). \tag{12}$$

As in the previous section, there is the obvious correspondence between the c-number variables and the operators.

It has been shown previously that, with coherent input at the lower frequency, we would expect to see an almost total conversion of the fundamental into the second harmonic, followed by a partial revival of the fundamental [5,28]. As well as this effect not being predicted by an analysis using linearisation of the operator equations of motion, the quantum statistical properties of the fields were found to be quite different from earlier predictions, at least for large effective interaction strengths. Here we wish to examine the effects of a thermal input on the output fields, which we would not expect to be amenable to a linearised analysis as the necessary condition of small fluctuations is not valid for thermal fields.

In Fig. 6 we show the mean values of the two fields for both coherent and thermal inputs at the fundamental. The normalised interaction strength used to plot the figures for SHG is defined as $\xi = \kappa|\alpha(0)|z/\sqrt{2}$. What is immediately visible is that a thermal input with the same mean photon number gives much greater mean conversion efficiency for shortish interaction lengths. We interpret this as being due to the fact that two photons must combine to produce one at the higher frequency and, in a thermal field, we find a high degree of photon bunching. Therefore, on average, the process proceeds more efficiently. What we also find, however, at an interaction length a little longer than that shown here, is that the revival of the fundamental is less complete than that found in [5], due to a lack of coherence between the fields traversing the crystal. It is also instructive to examine the intensity fluctuations in the two fields. As is known, and demonstrated in Fig. 7, with a coherent input the two fields exhibit sub-Poisso-

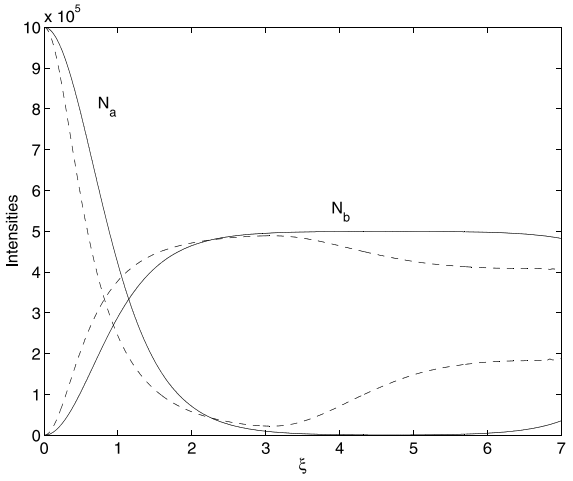

Fig. 6. The mean fields for travelling wave SHG, with coherent (solid lines) and thermal pumping (dashed lines), both with a mean value of $|\alpha(0)|^2 = 10^6$ and a value of $\kappa = 0.01$. The horizontal axis is in units of the normalised interaction strength, $\xi = \kappa|\alpha(0)|z/\sqrt{2}$. The results for coherent and thermal inputs used 7.6×10^5 and 1.8×10^5 stochastic trajectories, respectively.

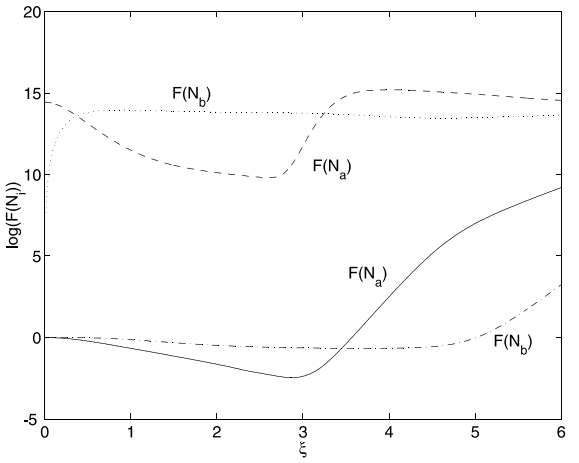

Fig. 7. The Fano factors for the two fields in travelling wave SHG, with coherent (upper pair of curves) and thermal inputs (lower pair of curves) as in Fig. 6. Note that the vertical scale is logarithmic.

nian photon statistics for some interaction lengths. This is seen as negative values of the logarithms of the Fano factors shown in the plot. In the thermal input case, although the fundamental exhibits less fluctuations than the input for some interaction lengths, it is always far from being Poissonian. The second harmonic also exhibits huge fluctuations. This indicates that, while a thermal input may give greater conversion efficiency, the outputs will exhibit huge intensity fluctuations. However, if we are interested in only the intensities rather than the quantum properties of the output fields, this would not be a problem.

4. Conclusion

We have shown how to treat optical parametric processes with different input states in a fully quantum mechanical manner and without serious restrictions as to maximum photon number, using as examples travelling wave second harmonic generation and the nondegenerate optical parametric amplifier in both stimulated and spontaneous modes of operation. Use of stochastic differential equations in the positive-P representation allows for the exact treatment of the coherent and thermal input states we have considered here. We find noticeable differences in the predictions for both the mean fields and the statistical behaviour, depending on the particular input states. In travelling-wave SHG, use of a thermal input allows for a greater average conversion efficiency, although at the expense of greater intensity fluctuations. In the NOPA, a thermal signal allows for greater two and four photon coincidence rates, which may prove useful for tests of the nonlocal properties of quantum mechanics, especially via the production of GHZ states. A thermal pump of high average intensity may be mimicked by passing an intense laser beam through a rotating disk of random index material before it enters the nonlinear crystal, so that our predictions should be easily amenable to experimental verification.

Acknowledgements

This research was supported by the New Zealand Foundation for Research, Science and Technology (UFRJ0001), the Brazilian agency CNPq (Conselho Nacional de Desenvolvimento Científico e Tecnológico) and the Deutsche Forschungsgemeinschaft.

References

[1] J.R. Armstrong, N. Bloembergen, J. Ducuing, P.S. Pershan, Phys. Rev. 127 (1962) 1918.
[2] Z.Y. Ou, Phys. Rev. A 49 (1994) 2106.
[3] R.D. Li, P. Kumar, Opt. Lett. 18 (1993) 1961.
[4] M.D. Reid, Phys. Rev. A 40 (1989) 913.
[5] M.K. Olsen, R.J. Horowicz, L.I. Plimak, N. Treps, C. Fabre, Phys. Rev. A 61 (2000) 021803.
[6] M.K. Olsen, L.I. Plimak, A.Z. Khoury, Phys. Rev. A (submitted).
[7] B.R. Mollow, R.J. Glauber, Phys. Rev. 160 (1967) 1076.
[8] B.R. Mollow, R.J. Glauber, Phys. Rev. 160 (1967) 1097.
[9] F.A.A. El-Orany, J. Peřina, M. Sebawe Abdalla, Opt. Commun. 187 (2001) 199.
[10] A. Kuzmich, I.A. Walmsley, L. Mandel, Phys. Rev. Lett. 85 (2000) 11349.
[11] G. Drobný, I. Jex, Phys. Rev. A 46 (1992) 499.
[12] G. Drobný, I. Jex, V. Bužek, Phys. Rev. A 48 (1993) 569.
[13] A. Bandilla, G. Drobný, I. Jex, Phys. Rev. A 53 (1996) 507.
[14] A. Bandilla, G. Drobný, I. Jex, Opt. Commun. 128 (1996) 353.

[15] A. Bandilla, G. Drobný, I. Jex, Opt. Commun. 156 (1998) 112.
[16] A. Bandilla, G. Drobný, I. Jex, J. Opt. B 2 (2000) 265.
[17] R.J. Glauber, Phys. Rev. 131 (1963) 2766.
[18] E.C.G. Sudarshan, Phys. Rev. Lett. 10 (1963) 277.
[19] P.D. Drummond, C.W. Gardiner, J. Phys. A 13 (1980) 2353.
[20] Z.Y. Ou, L. Mandel, Phys. Rev. Lett. 61 (1988) 50.
[21] P. Grangier, M.J. Potasek, B. Yurke, Phys. Rev. A 38 (1988) 3132.
[22] Z.Y. Ou, S.F. Pereira, H.J. Kimble, K.C. Peng, Phys. Rev. Lett. 68 (1992) 3663.
[23] C.W. Gardiner, Quantum Noise, Springer, Berlin, 1991.
[24] G.R. Grimmett, D.R. Stirzaker, Probability and Random Processes, Clarendon Press, Oxford, 1992.
[25] D.M. Greenberger, M.A. Horne, A. Zeilinger, in: M. Kafatos (Ed.), Bell's Theorem, Quantum Theory, and Conceptions of the Universe, Kluwer Academic Publishers, Dordrecht, The Netherlands, 1989, p. 73.
[26] A. Zeilinger, M.A. Horne, H. Weinfurter, M. Zukowski, Phys. Rev. Lett. 78 (1997) 3031.
[27] J.-W. Pan, M. Daniell, S. Gasparoni, G. Weihs, A. Zeilinger, Phys. Rev. Lett. 86 (2001) 4435.
[28] M.K. Olsen, L.I. Plimak, M.J. Collett, D.F. Walls, Phys. Rev. A 62 (2000) 023802.